Chinese Chemical Letters 34 (2023) 108285

Contents lists available at ScienceDirect

Chinese Chemical Letters

journal homepage: www.elsevier.com/locate/cclet

Engineering sulfur vacancies for boosting electrocatalytic reactions

Xianxu Chu[a], Yueyu Liao[b], Lu Wang[a], Junru Li[a], Hui Xu[b,*]

[a] Henan Key Laboratory of Biomolecular Recognition and Sensing, College of Chemistry and Chemical Engineering, Shangqiu Normal University, Shangqiu 476000, China

[b] Key Laboratory of Advanced Catalytic Materials and Technology, Advanced Catalysis and Green Manufacturing Collaborative Innovation Center, Changzhou University, Changzhou 213164, China

ARTICLE INFO

Article history:
Received 22 December 2022
Revised 20 February 2023
Accepted 1 March 2023
Available online 5 March 2023

Keywords:
Sulfur vacancy
Electrocatalytic reactions
Functionalities
Surface properties
Energy conversion

ABSTRACT

Transition metal sulfides are demonstrated to play an increasingly important role in boosting the deployment of ecofriendly electrocatalytic energy conversion technologies. It is also widely recognized that the introduction of vacancies is now becoming an important and valid approach to promote the electrocatalytic performance. In this review, the significance of sulfur vacancies on the enhancement of catalytic performance *via* four main functionalities, including tuning the electronic structure, tailoring the active sites, improving the electrical conductivity, and regulating surface reconstruction, is comprehensively summarized. Many effective strategies for the sulfur vacancy engineering, such as plasma treatment, heteroatom doping, and chemical reduction are also comprehensively provided. Subsequently, recent achievements in sulfur vacancy fabrication on various hotspot electrocatalytic reactions are also systematically discussed. Finally, a summary of the recent progress and challenges of this interesting field are organized, which hopes to guide the future development of more efficient metal sulfide electrocatalysts.

© 2023 Published by Elsevier B.V. on behalf of Chinese Chemical Society and Institute of Materia Medica, Chinese Academy of Medical Sciences.

1. Introduction

The rapid development of economy and society stimulates researchers to explore more energy sources. Currently, large proportions of these energy sources are derived from traditional fossil fuels, such as oil, coal, natural gas, resulting in environment deterioration and energy crisis [1,2]. Therefore, exploiting sustainable and feasible energy conversion or storage devices to decrease the dependence on fossil fuels and alleviating the ever-increasing environmental pollution is becoming increasingly critical [3,4]. Sustainable energy conversions are widely recognized as promising technologies for producing energy sources, and many advanced energy conversion technologies have been successfully developed in recent years, such as fuel cells [5–8], water electrolysis [9,10], metal-air batteries [11], featuring with high energy conversion efficiency and environmental benignity, which can be potentially employed in the portable devices and commercial vehicles. It should be noted that electrocatalyst is the crucial component of these advanced energy conversions, which is demonstrated to be effective for lowering the activation energy barrier for catalytic reactions [12,13]. However, some challenging issues should also be addressed to promote the catalytic performance of catalysts and further boost the widespread applications of energy conversion devices and thereby break away from the dependence on traditional fossil fuel.

According to the electrocatalytic reaction mechanisms, it is clearly found that the catalytic performance of an electrocatalyst is associated with its intrinsic electronic structure and surface properties, where an electrocatalyst with intrinsically favorable electronic configuration will benefit for the optimization of the binding strength with intermediates [14,15]. Additionally, fabricating a catalyst with modified surface properties will endow them with rich catalytically active sites, which will thus facilitate the catalytic reactions by providing a full contact area [16–18]. Bearing these two concepts into considerations, intensive research efforts have been dedicated to the modification of electrocatalysts *via* electronic configuration and geometric structure engineering.

In recent years, defect engineering has been reported to be a promising strategy to adjust the electronic configuration of catalyst, which may thus afford a chance to obtain outstanding electrocatalytic performance [19]. In general, defect sites in electrocatalysts are usually unique electronic structure that can properly combinate with reaction intermediates to deliver enhanced catalytic activity and durability. In addition, it should also be noted that defect engineering can effectively regulate the active sites *via*

* Corresponding author.
E-mail address: xuhui006@cczu.edu.cn (H. Xu).

https://doi.org/10.1016/j.cclet.2023.108285
1001-8417/© 2023 Published by Elsevier B.V. on behalf of Chinese Chemical Society and Institute of Materia Medica, Chinese Academy of Medical Sciences.

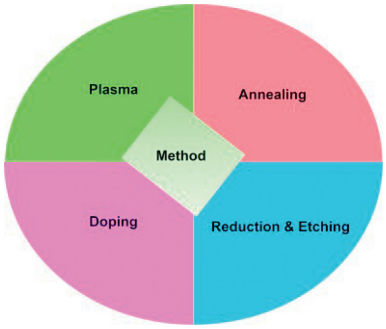

Scheme 1. Schematic illustration of the method for engineering sulfur vacancies.

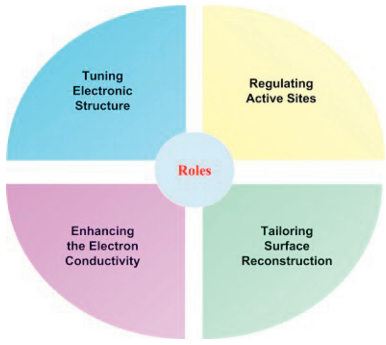

Scheme 2. Schematic illustration of the crucial roles of sulfur vacancies in electrocatalytic reactions.

increasing the density and optimizing the active sites [20,21]. Also, it is well recognized that the defect site engineering is beneficial for substantially improving the electrical conductivity, thereby accelerating the electron transfer during electrochemical reactions [22]. Additionally, defect site engineering has also confirmed to be effective for regulating the surface reconstruction of nanocatalysts and induce the formation of highly active species for further boosting the catalytic reaction [23].

Generally, defect includes anion vacancy, cation vacancies, metal defects and nonmetal defects. Among them, the anion vacancy, especially for oxygen vacancy and sulfur vacancy, have attracted increasing interest for boosting electrochemical reactions due to their unique properties [24]. In recent years, transition metal sulfides are emerging as promising candidates to substitute noble metals for boosting electrocatalytic reactions, due to their high intrinsic activity, multiple active sites, and tunable electronic configuration [25,26]. Most of all, the creation of sulfur vacancies in the metal sulfides will effectively tailor the physiochemical and electrochemical properties, which will thus endow them with distinguished electrocatalytic performance [27]. Inspired by this, tremendous efforts have been dedicated to the modification of metal sulfide catalysts *via* sulfur vacancy engineering, and their catalytic performance is substantially improved. However, a comprehensive review regarding the formation of sulfur vacancies, important roles of sulfur vacancies, and the application of sulfur-enriched catalysts for various hotspot electrocatalytic reactions is rarely reported.

Herein, we organized a comprehensive review about the sulfur vacancy engineering for boosting electrocatalytic reactions with specifical focus on the engineering strategies and roles of sulfur vacancies in electrochemical reactions. We discuss in detail the engineering strategies of sulfur vacancy and provide a comprehensive and timely research progress of sulfur vacancy engineering (Scheme 1) on regulating the catalytic properties of the hotspot electrochemical reactions of oxygen evolution reaction (OER), hydrogen evolution reaction (HER), nitrogen reduction reaction (NRR), CO_2 reduction reaction (CO_2RR), and oxygen reduction reaction (ORR). Additionally, we also discussed the effects of sulfur vacancy to tune electrocatalytic performance from four aspects and also presented a brief summary of this interesting field (Scheme 2), with ideas about the future directions and potential challenges.

2. Methods for creating sulfur vacancies

2.1. Plasma treatment

Plasma, the fourth state of matter, consists of various species including electrons, neutrals, excitons, and excited molecules generated at low or atmospheric pressures. The plasma species are more active than the ground-state atoms or molecules, which can thus show great advantages for enabling the fabrication of vacancy-enriched nanocatalysts [28]. Generally, it is demonstrated that the high-energy proton from plasma species tends to interact with anion than cation, and in that case, plasma treatment normally creates anion vacancy [29,30]. Moreover, the concentration of anion vacancy can be easily tailored by regulating the treatment time, irradiation time and intrinsic structure of the catalyst. Low-temperature plasma treatment represents a powerful tool for materials processing including defect engineering, surface modification, and have been successfully used for the production and modulation of electrode materials and electrocatalysts for energy storage and conversion technologies [31]. For instance, Wang *et al.* [32] reported the synthesis of low-cost $NiCo_2S_4$ and then processed using low-temperature plasma to further modify their electrochemical properties. By employing Ar low-pressure plasma treatment, surface reconstruction and phase changes are successfully achieved while tailoring the S-vacancy concentration. Moreover, it is also demonstrated that plasma-induced $NiCo_2S_4$ could also present the reduction of Ni and Co valence states and generate more sulfur vacancies.

Li *et al.* [32] also demonstrated that plasma treatment could also induce the formation of rich sulfur vacancies in MoS_2. As shown in Fig. 1a, they used remote hydrogen plasma to create sulfur vacancies on amorphous molybdenum sulfide, which leads to the substantial improvement in electrocatalytic HER performance. According to Fig. 1b, it is also uncovered that the surface of pristine amorphous MoS_x (a-MoS_x) on carbon cloth is hydrophobic (137°) but it becomes hydrophilic (7°) after H_2 plasma treatment. Moreover, it is also demonstrated that the hydrogen plasma treatment of a-MoS_x not only increases the active site density but also changes the surface energy of the catalysts (Figs. 1c and d), which results in inhibiting the bubble trapping on catalytic surfaces.

2.2. Annealing treatment

Typically, metal sulfides can be prepared *via* wet-chemical methods that employing metal salts as precursors and sodium thiosulfate, thioacetamide, and sodium sulfide as sulfur sources [33]. Besides, metal sulfides can also be synthesized *via* annealing treatment by using sulfur powders as sulfur source. Some sulfur atoms would be released during the high-temperature annealing treatment, leading to the formation of high-quality metal sulfides with rich sulfur vacancies [34,35]. For example, Voiry *et al.* [36] have investigated the role of sulfur vacancies in MoS_2 on the electrocatalytic performance of HER. Specifically, they have introduced the sulfur vacancies in the 2H-MoS_2 lattice *via* annealing the nanosheets under H_2 atmosphere from 400 °C up to 800 °C. After annealing under hydrogen atmosphere, additional defects in the form of sulfur atom vacancies are clearly observed in the MoS_2 basal planes (Fig. 2a). More importantly, it is also uncovered that the MoS_2 signatures decrease when increasing the annealing

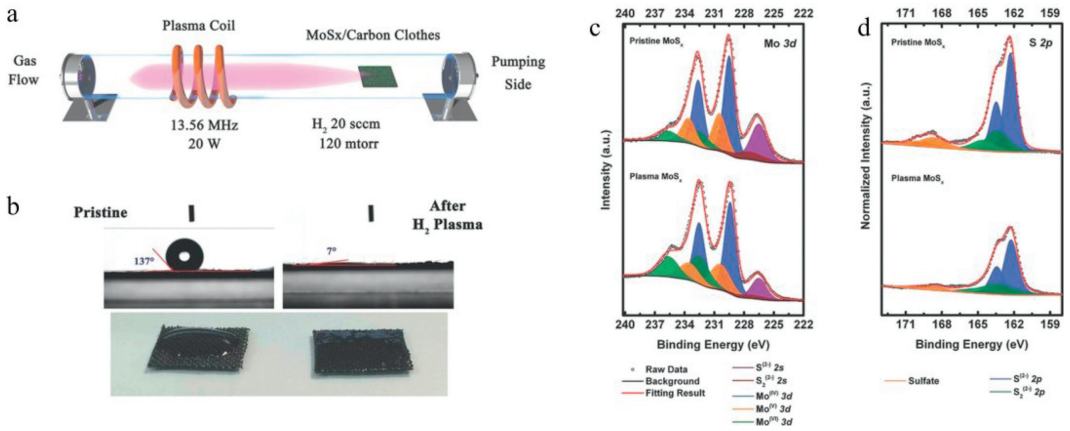

Fig. 1. (a) Schematic illustration for H_2 plasma treatment of a-MoS_x. (b) The contact measurement and the photo for contact behaviors of water droplets to pristine and H_2 plasma treated a-MoS_x. XPS spectra of the (c) Mo 3d and (d) S 2p of a-MoS_x before and after H_2 plasma treatment. Reproduced with permission [32]. Copyright 2016, Wiley-VCH.

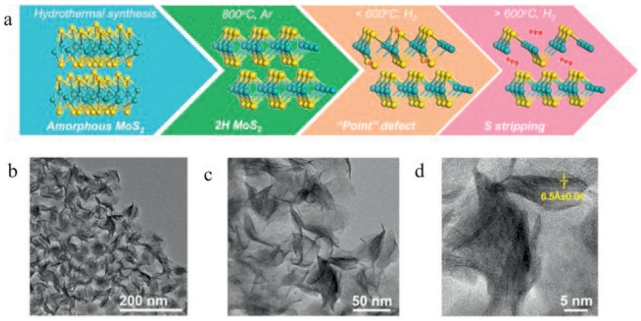

Fig. 2. (a) Evolution of the different structures of MoS_2 that prepared *via* different methods. (b) TEM images of the MoS_2. (c, d) High-resolution TEM images of the stacked individual layers of the as-synthesized MoS_2. Reproduced with permission [36]. Copyright 2019, American Chemical Society.

temperatures under hydrogen (Figs. 2b-d). This work has confirmed the great significance of annealing treatment for the construction of sulfur vacancies in the sulfides.

2.3. Heteroatom doping

Heteroatom doping of transition metal sulfides has drawn great interest because of its applicability to the modulation of their electrical and optical properties [37–39]. In addition, it is also reported that heteroatom doping can regulate the electronic structure of lattices to improve the electrical conductivity and provide additional active sites. Taking Qian's work as a representative example [40], they have reported the synthesis of the P_y-FeS_{2-x} with abundant sulfur vacancies *via* P doping (Fig. 3a). Specifically, the Pre-Fe microflowers containing abundant nanosheets are firstly prepared, and then converted into FeS_2 microflowers *via* sulfidation treatment. Finally, P atoms were doped into FeS_2 lattice and *in-situ* formed the sulfur vacancies under a low-temperature phosphating process. Owing to the difference of P and S in electronegativity, P atom was easily bonded with Fe atom and thus occupied the location of S atoms, thereby yielding abundant sulfur vacancies.

Incorporating metal ions to replace the host metal ions in the sulfides can also create sulfur vacancies. As demonstrated by Chen's work [41], they have proposed an effective method for constructing sulfur vacancies modulated SnS_2 nanoflower by Cu doping (Fig. 3b). It was uncovered that Cu doping could replace the position of Sn and favors for introducing sulfur vacancies in SnS_2, which thus afforded a potential method for synthesizing sulfur vacancy modified electrocatalysts.

2.4. Chemical reduction

Plasma treatment frequently needs high temperature and a large amount of gas, which is not conducive to environmental protection in the perspective of energy consumption. Developing moderated method for creating sulfur vacancies is urgently sought. In recent years, chemical reduction method is emerging as an effective strategy for creating the sulfur vacancies for boosting electrocatalytic reactions, where the reductants can reduce the oxidation states of the metal cations to form the anion vacancies through the charge neutrality of the crystal [42]. Generally, the widely utilized reducing agents include N_2H_4, $NaBH_4$, H_2, NH_3, CaH_2 and NaH [43]. In general, moderate reduction with $NaBH_4$ has been proved to be a facile, low-energy consumption and safe method to introduce defects into the materials. $NaBH_4$ can be used as a scavenger at room temperature to remove the sulfur atom from metal sulfides with the merit of its reducibility. In general, the specific reaction mechanisms can be illustrated as the following equation:

$$8M^{n+} + NaBH_4 + 2H_2O \rightarrow 8M^{(n-1)+} + NaBO_2 + 8H^+ \quad (1)$$

Taking Chen's work as an example [24], they have reported the synthesis of reduced graphene oxide (rGO) supported sulfur-vacancy-enriched $FeNi_2S_4$ nanocrystals through a facile chemical reduction method. It is demonstrated that the introduction of $NaBH_4$ can significantly create the amount of sulfur vacancies, and the possible reaction is also presented as the following equation:

$$4FeNi_2S_4 + xNaBH_4 + 2xH_2O \rightarrow 4FeNi_2S_4 + xNaBO_2 + 4xH_2S \quad (2)$$

Xu *et al.* [44] also reported a low-cost and mild $NaBH_4$ reduction method can conveniently fabricate the $NiCo_2S_4$-based materials to deliver superb electrochemical performance.

2.5. Electrochemical etching

Electrochemical etching has recently demonstrated to be a promising strategy for creating metal defects in nanocatalysts to boost electrochemical reactions, due to the dissolution of metal ions [45–47]. However, anion vacancies creation by electrochemical etching method has been rarely reported. Recently, previous works have reported that inert and stable sulfur atoms can be hydrogenated and removed *via* electrochemical treatment under appropriate potentials. For example, Tsai *et al.* [30] created the

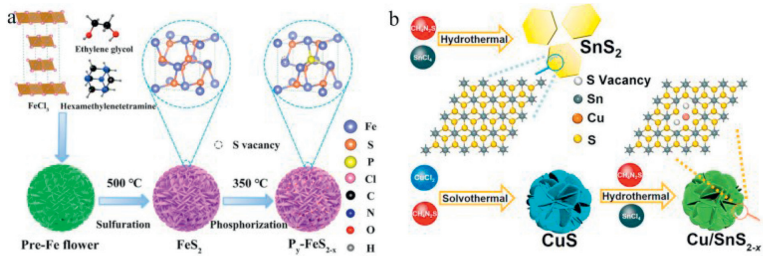

Fig. 3. Schematically showing the formation of sulfur vacancies *via* heteroatom doping. (a) Scheme of the synthesis of P_y-FeS_{2-x}. Reproduced with permission [40]. Copyright 2022, Elsevier. (b) Scheme of the synthesis of Cu/SnS_{2-x}. Reproduced with permission [41]. Copyright 2021, Elsevier.

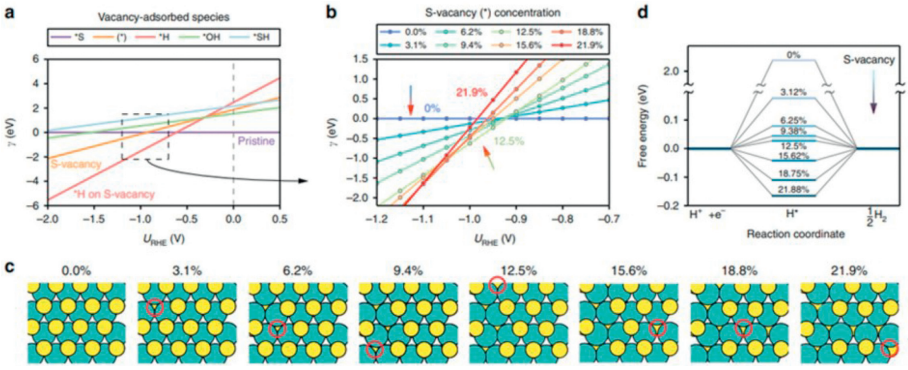

Fig. 4. (a) Surface energy per unit cell for 2H-MoS_2 as a function of applied potential for the basal plane of 2H-MoS_2 with different adsorbate species at a fixed sulfur vacancy (3.1%). (b) Surface energy per unit cell for a range of S-vacancy concentrations, without any adsorbates. (c) Scheme for the instability of sulfur vacancies when they are existed in succession. (d) Free energy diagram for the HER on S-vacancy sites. Reproduced with permission [30]. Copyright 2017, Nature Publishing Group.

sulfur-vacancy on the basal plane of the 2H-MoS_2 *via* an innovative electrochemical method. They have disclosed that the sulfur atoms on the basal plane can be electrochemically reduced under accessible applied potentials, where the sulfur atoms can be hydrogenated and then removed as H_2S gas to generate S-vacancies (Figs. 4a and b). More interestingly, it is also demonstrated that the concentration of sulfur vacancies can be well varied by altering the applied desulfurization potential. Additionally, this method could also be extended to the generation of S-vacancies on multilayered MoS_2 supported on flat carbon rods and porous carbon foam, leading to the substantial improvement in electrocatalytic HER performance (Figs. 4c and d).

3. Characterizations of sulfur vacancy

With the rapid development of material science and technology, the material characterizations, especially for surface defect characterization techniques have been substantially improved, the mystery of microstructure in materials has been gradually revealed. For the characterization of sulfur vacancies, many advanced characterization methods have been well developed, which can be mainly divided into two categories. One is the spectroscopy method, which can identify the surface structure changes of materials by analyzing the spectroscopy signal [34]. The other is associated with the microscopic imaging technology [35].

3.1. Spectroscopy characterization methods

X-ray photoelectron energy spectrum (XPS) is one of the most important characterization techniques for analyzing the surface defect of catalysts, which has also been widely used for the characterizations of sulfur vacancies by analyzing the surface chemical valence and bonding information of sulfides [48]. Raman spectroscopy is also used to achieve the surface chemical bonds' vibration signal of materials to investigate the surface structure of catalyst, where the defects inducing the change of surface chemical bond energy can well be detected by the Raman spectroscopy. In recent years, the X-ray adsorption fine spectroscopy (XAFS) is also obtained to gain a better understanding on the atomic coordination environment and chemical bond length of catalyst, which is also beneficial for analyzing the sulfur vacancies of catalyst [49,50]. Besides these important techniques, the electron paramagnetic resonance spectroscopy (EPR) is one of the most important techniques for characterizing the defect structures, especially for oxygen defects and sulfur vacancies in catalysts by measuring the resonance response signal of unpaired electrons in materials in the applied magnetic field [36].

3.2. Microscopic imaging characterization methods

In addition to the spectroscopy methods, microscopic imaging technology is also used for the characterizations of sulfur vacancies [51,52]. Microscopic imaging technology mainly included the scanning electron microscope (SEM), transmission electron microscope (TEM), atomic force microscope (AFM), and scanning tunneling microscope (STM). STM and TEM are often used to study the atomic defect structure of catalysts with a high resolution. The high-angle annular dark field-scanning transmission electron microscopy HAADF-STEM images can characterize the local defect structure and defect distribution on the surface of the catalyst, which can help analyze the surface atomic arrangement of the catalyst and thus characterize the surface sulfur vacancies of sulfides.

4. Roles of sulfur vacancies

The electronic structures are demonstrated to play a critical role in tuning the electrocatalytic performance of nanocatalysts, and this can be modified by heteroatom doping [53], defect engineering [54], interface engineering [55], and so on. After tailoring the electronic structure, the spin and charge will be redistributed,

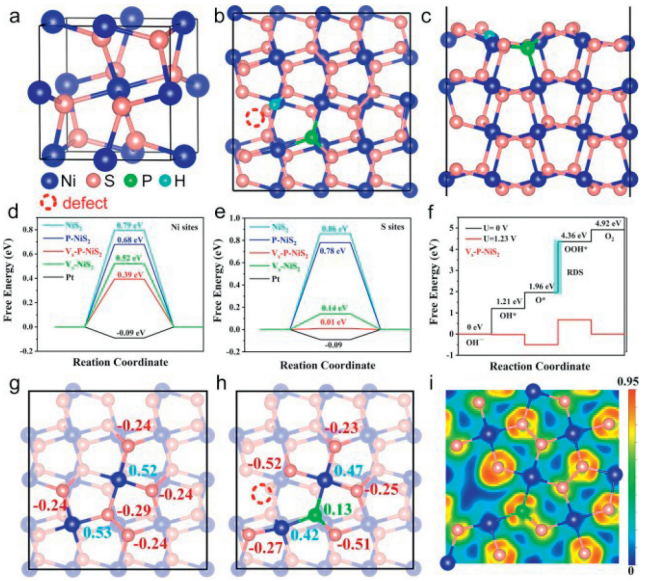

Fig. 5. (a) The crystal structure of NiS_2 with a typical pyrite-type phase. (b, c) The optimized model for hydrogen adsorption at the S sites of sulfur vacancy-enriched P-NiS_2 (V_s-P-NiS_2). HER free energy diagram for different (d) Ni sites and (e) S sites. (f) The calculated Gibbs free-energy diagram for four steps of OER on V_s-P-NiS_2. The Bader charge numbers of atoms in (g) NiS_2 and (h) V_s-P-NiS_2. (i) Charge density distribution of V_s-P-NiS_2. Reproduced with permission [58]. Copyright 2021, Elsevier.

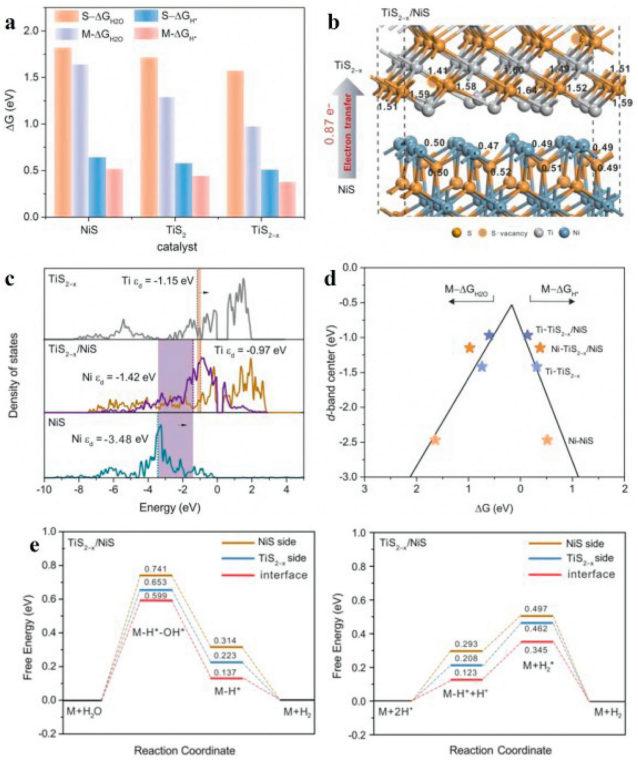

Fig. 6. (a) The calculated free energy for alkaline HER on the S site (S-ΔG_{H_2O} and S-ΔG_{H^*}) and metal (Ti or Ni) sites, (M-ΔG_{H2O} and M-ΔG_{H^*}) of the NiS, TiS_2 and TiS_{2-x} catalysts. (b) Bader charge analysis of S cations *via* a TiS_{2-x}/NiS heterointerface inside the TiS_{2-x}/NiS catalysts. (c) Partial density of states (DOS) curves and d-band centers (ε_d) of different catalysts. (d) Volcano plot based on the relationship between d-band centers and the calculated free energies of hydrogen adsorption and water dissociation on the metal (Ti or Ni) sites (M-ΔG_{H2O} and M-ΔG_{H^*}) of the NiS, TiS_{2-x} and TiS_{2-x}/NiS catalysts. (e) The free energy diagrams of the TiS_{2-x}/NiS catalyst for alkaline and acidic HER on the TiS_{2-x} side, the NiS side, and the TiS_{2-x}/NiS heterointerface. Reproduced with permission [61]. Copyright 2022, Elsevier.

leading to the significantly enhanced catalytic performance. As is well known to all, vacancies can regulate the stoichiometric ratio and lead to the distortion of electric field, thus resulting in a variation of the electronic distribution [56,57].

4.1. Tuning the electronic structure

Particularly, the introduction of sulfur vacancies into sulfides can induce the cracking of crystal, modulate the atomic structure and subsequently realize the electronic structure regulation, all of which are demonstrated to be beneficial for the substantial improvement in electrocatalytic performance. For instance, the sulfur vacancies created on the basal plane of 2H-MoS_2 can expose under-coordinated edge sites and induce a more disorder structure, thereby leading to the optimization of the adsorption free energy of hydrogen (ΔG_{H^*}) and improved HER catalytic activity. Chen *et al.* [58] demonstrated that the sulfur-vacancies defect engineering in the NiS_2 could significantly modulate its electronic structure to elevate the electrocatalytic HER and OER performance by simultaneously optimizing ΔG_{H^*} and oxygen-containing intermediates (OH*, O* and OOH*) (Figs. 5a-f), which have further confirmed significance of sulfur vacancy engineering on the substantial improvement in electrocatalytic performance (Figs. 5g-i).

4.2. Regulating the active sites

Active sites for a certain catalyst mean the position where electrochemical reactions occur. Introducing vacancies on the electrocatalysts thus played a crucial role in affecting the catalytic performance *via* following two strategies. (1) Increase the number of catalytic active sites; introducing vacancies can activate some inactive metal sites to work as highly active sites to boost electrochemical reactions, which will lead to an increase of overall density of active sites [59]. (2) Regulate the intrinsic activity of each active site; introducing vacancies is also an effective method for substantially enhancing the overall catalytic activity by improving the intrinsic activity of each active site. For example, Xu *et al.* [60] demonstrated that the creation of sulfur vacancies in the spinel-type Co_3S_4 can significantly regulate the active sites to boost electrocatalytic OER. Yang *et al.* [61] reported the synthesis of non-stoichiometric TiS_{2-x}/NiS heterostructure that comprised of abundant sulfur vacancies (Fig. 6). By integrating DFT calculations and experimental results, it is uncovered that the existence of rich sulfur vacancies and multiple active sites could effectively regulate the d-electronic structure of the metal Ti and Ni atoms, thereby achieving an optimized binding strength with H* and delivering outstanding electrocatalytic HER performance.

4.3. Enhancing the electrical conductivity

For synthesized electrocatalysts, electron conductivity can greatly accelerate the electron transfer during electrochemical process, and the existence of sulfur vacancies in the constructed electrocatalysts can significantly improve the electron conductivity to accelerate electron transfer [62–64], improving the catalytic activity accordingly. The generated sulfur vacancies in the metal sulfides can form new defect states near the band gap and the conduction band can thus be easily activated by the two electrons close to the sulfur vacancies and thus the electrochemical resistance decreased [65]. Theoretical calculations reveal that the localized electrons with the neighboring sulfur vacancies will be delocalized to easily facilitate the electron transport from the reaction interfaces to electrodes [66,67]. Besides, sulfur vacancies can act as an electronic charge carrier to greatly improve the intrinsic electrical conductivity of metal sulfide, they can also create more active sites for catalytic reactions, allowing for a fast redox reaction. For

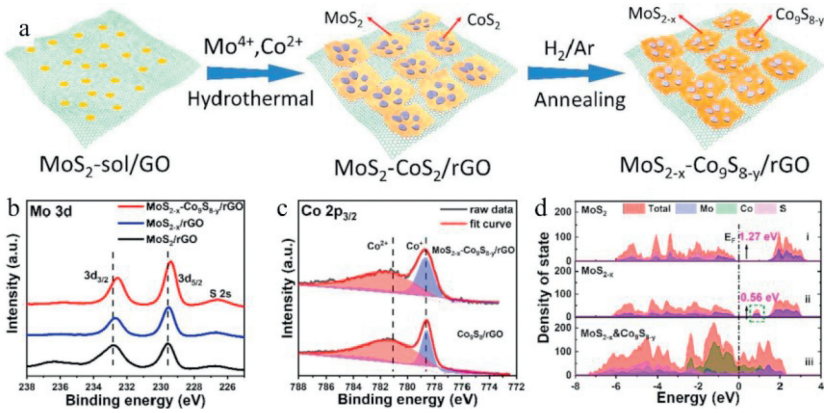

Fig. 7. (a) Schematic illustration for the synthesis of MoS_{2-x}-Co_9S_{8-y}/rGO. XPS spectra of the (b) Mo 3d and (c) Co $2p_{3/2}$ of MoS_{2-x}-Co_9S_{8-y}/rGO and referenced samples. (d) Density of state of MoS_2, MoS_{2-x}, and MoS_{2-x}&Co_9S_{8-y}. Reproduced with permission [68]. Copyright 2022, Elsevier.

example, Huang *et al.* [68] synthesized the covalent MoS_2-Co_9S_8 heterostructure loaded on the surface of RGO with rich sulfur vacancies in both MoS_2 and Co_9S_8 (Fig. 7a). According to a series of Mo 3d XPS spectra (Fig. 7b), it is discovered that the Mo 3d peaks of MoS_{2-x} shift to lower binding energy due to the sulfur vacancy, resulting in enriched electron cloud densities around Mo and reduced valence states of Mo. In addition, a higher Co^+/Co^{2+} of MoS_{2-x}-Co_9S_{8-y}/rGO than the Co_9S_8/rGO (0.62 *vs.* 0.36) also confirms the successful formation of S vacancy in Co_9S_8 (Fig. 7c). Moreover, the density of state (DOS) model of MoS_{2-x} presents a remarkable rearrangement of states of MoS_2, generating a donor level in the forbidden band region between the conduction and valence bands (Fig. 7d). Consequently, electrons in the valence band can leap to the defect level and form hole carriers, increasing the carrier concentration while also lowering the transition barrier of electrons to the conduction band, which greatly improves the electronic conductivity. Therefore, it is uncovered that sulfur vacancy and can significantly improve the electrical conductivity of sulfides.

4.4. Tailoring the surface reconstruction

For electrochemical reactions, surface reconstruction normally takes place and plays a crucial role in determining the electrocatalytic performance of nanocatalysts. Introducing vacancies into electrocatalysts has been reported to be recognized as an effective method for improving the catalytic performance [69,70]. Recent works have witnessed that vacancies can effectively tailor the surface reconstruction to further elevate the electrocatalytic performance [71–76]. For example, Shi *et al.* [77] synthesized the Co_9S_8 having rich sulfur vacancies (S_v-Co_9S_8) *via* Ar-plasma treatment for enhanced alkaline HER (Figs. 8a-d). By comparing with pristine Co_9S_8, the V_s-Co_9S_8 after experiencing alkaline HER pretreatment can exhibit much higher electrocatalytic activity and lower charge transfer resistance. During HER process, V_s can induce partial dissolution of sulfur on the surface, thereby leading to the formation of $Co(OH)_2$, which demonstrate a strong synergistic effect with the still-existing sulfur vacancies in optimizing the hydrogen adsorption (Figs. 8e and f). Additionally, the water dissociation promoted by the $Co(OH)_2$ and excellent electron conductivity stemmed from the S_v-Co_9S_8 synergistically contributed to the enhanced HER performance. Therefore, sulfur vacancies played a crucial role in tailoring the surface reconstruction to substantially improve the electrocatalytic performance.

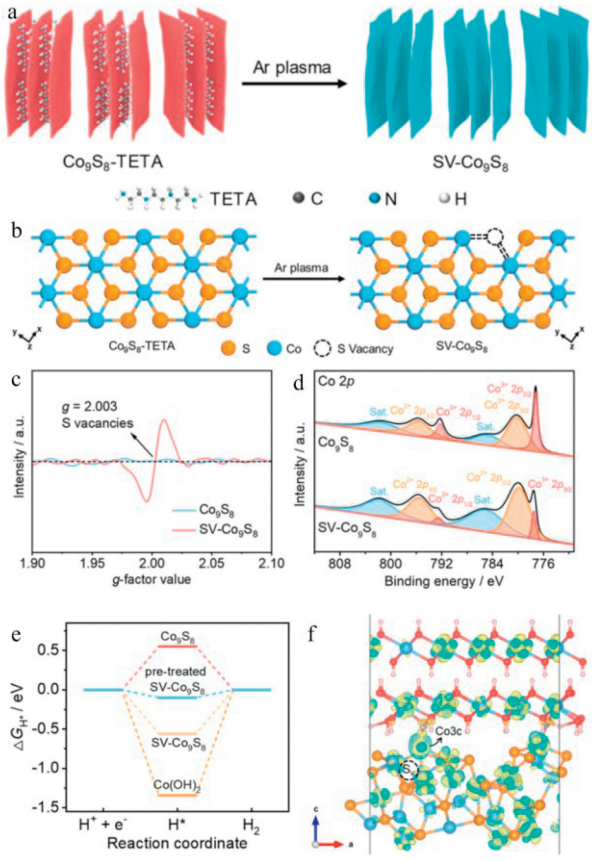

Fig. 8. (a, b) Schematic illustration of the preparation of S_v-Co_9S_8 and the formation of sulfur vacancies in Co_9S_8. (c) EPR and (d) XPS spectra of the Co_9S_8 and S_v-Co_9S_8. (e) Free energy diagrams of the HER and referenced catalysts. (f) Charge density difference analysis of pretreated S_v-Co_9S_8. Reproduced with permission [77]. Copyright 2022, American Chemical Society.

5. Sulfur vacancy-based catalysts for electrocatalytic reactions

5.1. Hydrogen evolution reaction

Electrochemical water splitting holds great promise for the sustainable hydrogen production [78–82]. Pursuing highly active and stable electrocatalysts for boosting electrochemical water splitting to generate H_2 has thus attracted much attention [83,84]. To date,

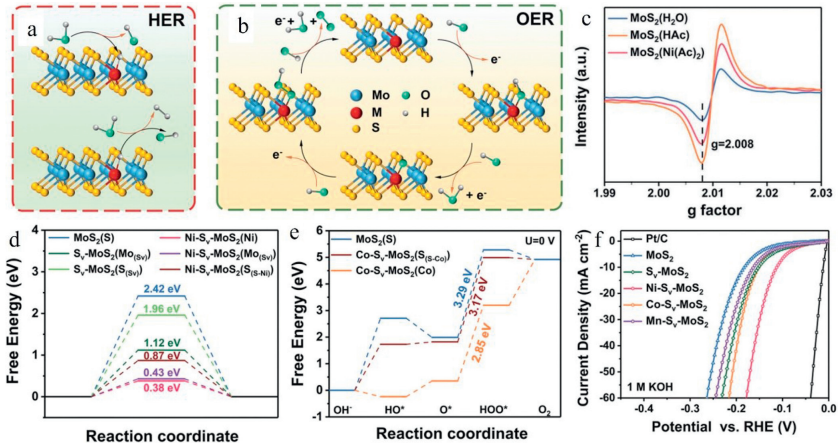

Fig. 9. (a) HER and (b) OER under alkaline conditions on metal-doped sulfur vacancy enriched MoS_2 (M-S_v-MoS_2). (c) EPR spectra of MoS_2 catalysts. (d) Adsorption free energy of H* on S sites in the basal plane of MoS_2, S, and Mo sites in S_v-MoS_2, and S, Ni, Mo sites in Ni-S_v-MoS_2. (e) Adsorption free energy of oxygen intermediates on S sites in the basal plane of MoS_2, and on the S and Co site in Co-S_v-MoS_2. (f) HER polarization curves of different electrocatalysts. Reproduced with permission [42]. Copyright 2022, Wiley-VCH.

Pt-based nanomaterials could exhibit the best catalytic performance for HER with the lowest overpotential and smallest Tafel plots [85–88]. However, the high cost and low natural reserves have seriously hampered their widespread applications. Exploring efficient and low-cost HER electrocatalysts as alternatives to substitute Pt-group noble metals is highly important [89–92]. In recent years, various noble-metal-free nanocatalysts have been well developed for boosting HER, and vacancy engineering has been reported to be one of the most effective strategies. As one of the most promising HER electrocatalysts, sulfides, particularly for MoS_2 with abundant sulfur vacancies [93,94], have been uncovered to be highly active towards HER, due to the presence of rich active sites that originated from creation of sulfur vacancies. Huo *et al.* [42] have confirmed that the introduction of in-plane sulfur vacancies and 3d transition metal dopants in concert could effectively activate the basal planes of MoS_2, and thus achieve outstanding electrocatalytic HER performance (Figs. 9a and b). The EPR spectra confirmed that the as-prepared MoS_2 possessed abundant sulfur vacancies (Fig. 9c). Upon DFT calculations, it is uncovered that the strong electronic coupling between metal dopants and host MoS_2 can synergistically reduce the ΔG_{H^*} and oxygen intermediate adsorption on the exposed active sites to boost electrocatalytic performance (Figs. 9d and e). As a result, the as-prepared MoS_2 catalyst can exhibit superb catalytic performance towards HER and OER (Fig. 9f).

Besides MoS_2 catalysts, sulfur vacancy can also enable other sulfides to be promising electrocatalysts towards HER. For instance, Yu *et al.* [95] synthesized the Mo-doped NiS/Ni_3S_2 polymorph heterostructure with plentiful sulfur vacancies (Figs. 10a and b). Deep investigations revealed that the sulfur centers on the Ni_3S_2 side of the nickel sulfide polymorphs are serving as the H_2-evolving sites, while the Ni sites on the Mo-NiS side are favorable for cleaving the HO-H bond (Fig. 10c). More importantly, theoretical calculations disclosed that the rich sulfur vacancies can expedite the evolution of H* to molecular H_2, thereby promoting the HER kinetics (Figs. 10d-f). Remarkably, the optimal Mo-NiS/Ni_3S_2 polymorph electrocatalyst could display the outstanding HER activity and excellent durability in alkaline solution, with the overpotentials of 73 and 230 mV at 10 and 100 mA/cm^2, respectively.

5.2. Oxygen evolution reaction

OER is a key process for various energy conversion technologies, such as metal-air battery and water-splitting for hydrogen production, resulting in tremendous attention to optimize OER in recent decades [96–98]. Compared with HER, OER is more complicated, which involves a 4-electron pathway and leads to sluggish reaction kinetics [99–101]. In recent years, many noble-metal-free electrocatalysts have also been developed and designed for boosting OER process *via* reducing the reaction energy barriers [102–106]. Also, anion vacancies, especially for oxygen vacancies have been proofed to be favorable for promoting the catalytic OER performance, which thus attract increasing attention [107–110]. Besides oxygen vacancies, sulfur vacancies are also reported to play a crucial role in affecting the electrocatalytic OER performance by modulating the electronic properties and/or increase exposed active sites of catalysts. In general, introducing sulfur vacancies can modify the electronic structure and regulate the oxygenated intermediate formation, which greatly promote the charge transfer and facilitate the exposure of catalytic active sites, thus resulting in substantial improvement in electrocatalytic performance [111]. Xu *et al.* [60] proposed the synthesis of spinel Co_3S_4 with rich sulfur vacancies, where the introduced sulfur vacancies can effectively delocalize the Co neighboring electrons and expose more Co^{2+} sites in spinel Co_3S_4 (Figs. 11a and b), lowering the charge transfer resistance and facilitate the generation of Co^{3+} active sites during the preactivation process. As a result, the sulfur-vacancy-enriched Co_3S_4 nanocatalyst can exhibit superb catalytic performance towards OER, which can exhibit low overpotential and small Tafel slope (Fig. 11c).

Chen and coworkers [112] also synthesized the sulfur-vacancy-enriched Co_3S_4 nanocatalyst to deliver superb catalytic performance towards OER. Specifically, the Co precursor grown on the nickel foam (NF) was prepared *via* a facile hydrothermal process. Subsequently, the Co_3S_4/NF was then obtained *via* sulphuration step, and after a method of $NaBH_4$ etching, the sulfur-vacancy-enriched V_s-Co_3S_4/NF was finally prepared. According to a series of electrochemical measurements and mechanism studies, it was disclosed that the introduction sulfur vacancy can efficiently alter the electron structure around the reactive sites, thereby promoting the adsorption of oxygen-involved intermediates. As expected, the V_s-Co_3S_4/NF could exhibit outstanding electrocatalytic performance towards OER, with an ultralow overpotential of 245 mV at 100 mA/cm^2.

5.3. Nitrogen reduction reaction

Electrochemical synthesis of NH_3 *via* NRR appeals considerable attention due to its fascinated merits, including moderate reaction condition, abundant reactants, and environmental friendliness

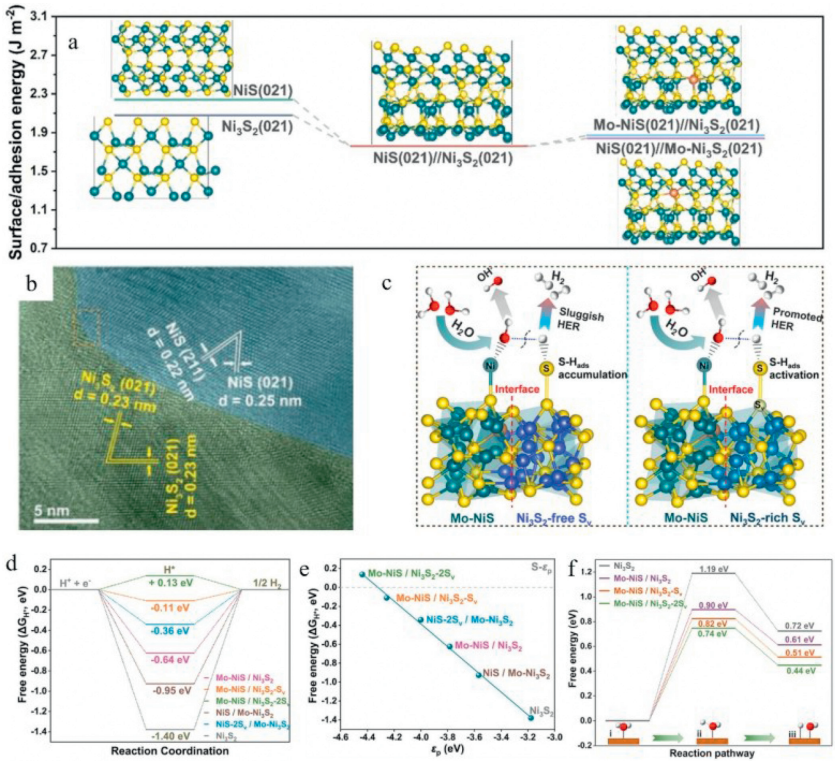

Fig. 10. (a) Surface/adhesion energy diagrams of different atomic models. (b) HRTEM image of the Mo-NiS/Ni_3S_2 polymorph electrocatalyst. (c) Schematic diagram illustrates the heterointerface and S-vacancy roles on the surface of the Mo-NiS/Ni_3S_2-free S_v (left) and rich S_v (right) electrocatalysts toward HER electrocatalysis. (d) HER free-energy diagram calculated for different catalysts. (e) Dependence of free energies of hydrogen adsorption on the p-band centers (ε_p) of S 3p state. (f) Reaction energy of water dissociation for different electrocatalysts. Reproduced with permission [95]. Copyright 2023, Elsevier.

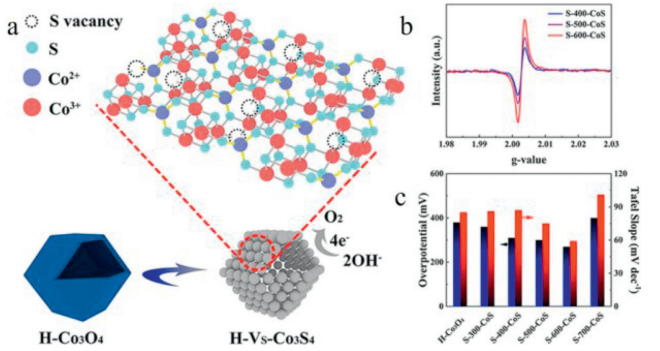

Fig. 11. (a) Schematic illustration of creation of sulfur-vacancy-enriched Co_3S_4 nanocatalyst. (b) EPR spectra of different electrrocatalysts. (c) Histograms of the overpotentials of different catalysts at 10 mA/cm^2 and the Tafel slopes. Reproduced with permission [60]. Copyright 2022, American Chemical Society.

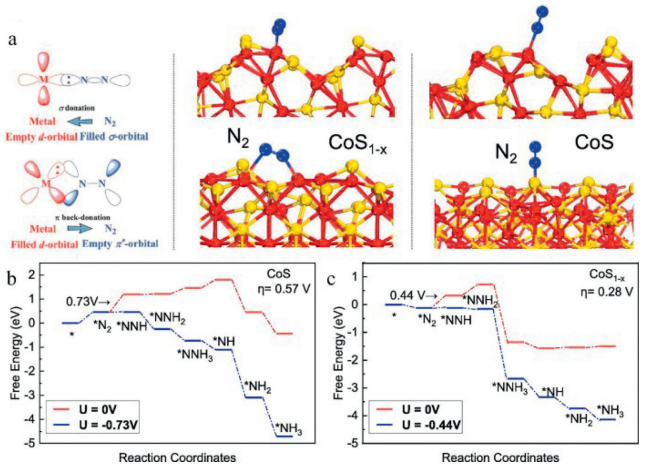

Fig. 12. (a) Scheme of N_2 bonding to metal atoms. Optimized geometry of N_2 adsorption on CoS_{1-x} and CoS surface. Gibbs free energy diagrams of distal pathways for NRR on (b) CoS and (c) CoS_{1-x} surface at different potentials. Reproduced with the permission [120]. Copyright 2021, Elsevier.

[113,114]. However, as well known, N≡N triple bond is difficult to split, thus, to realize the synthesis of advanced electrocatalysts to effectively split the N≡N triple bond is highly important [115–117]. Besides, the NRR electrocatalysis is also plagued by the competitor HER occurring in aqueous electrolyte during NRR process, hence, the selective adsorption of N_2 molecules on active sites to effectively regulate HER is prominently vital for a superb HER electrocatalyst. Similar to electrocatalytic HER, noble metals (Pd, Au, Ru and Rh) are still the benchmarked catalysts for NRR. However, the high cost and limited natural abundance have severely hindered their widespread applications [118]. Therefore, exploring inexpensive transition metal compounds is highly appreciated for boosting electrocatalytic NRR. Very recently, manufacturing oxygen or sulfur vacancies in electrocatalysts to effectively catalyze NRR have been extensively researched due to the tailored electronic structure, surficial configuration and selective chemisorption of molecules [119]. As a result, the intrinsic activity and electronic conductivity are significantly enhanced.

For example, Yang *et al.* [120] rationally synthesized the CoS nanoflowers with rich sulfur vacancies *via* Ar-plasma treatment. As well known, plasma can induce free electrons, energetic photons, reactive and radical species, which can break up the Co-S bond to generate sulfur vacancies at the edge sites of CoS (Fig. 12a). Benefitting from the existence of sulfur vacancies, the CoS nanoflower

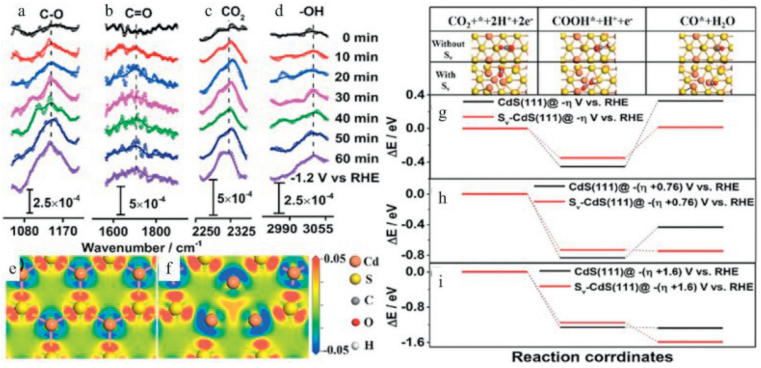

Fig. 13. (a-d) *In-situ* infrared absorption spectroscopy with attenuated total reflection mode analyses of CdS-CNTs for CO_2RR. The distribution of electron deformation density of (e) CdS(111) without S_v and (f) CdS(111) with S_v. (g-i) DFT calculation results of relative energy for possible intermediates during CO_2RR on CdS (111) without S_v and CdS (111) with S_v at different potentials. Reproduced with the permission [128]. Copyright 2019, Elsevier.

catalyst can yield a faradaic efficiency of 16.5%±1.5% and NH_3 production rate of 12.1±1.4 μg_{NH3} h^{-1} mg_{cat}^{-1} at −0.15 V *vs.* RHE. Theoretical calculations revealed that the sulfur vacancies could promote the N_2 chemisorption and lower the Gibbs free energy for N_2 protonation (Figs. 12b and c). Sun and coworkers [121] also demonstrated that the introduction of sulfur vacancies could facilitate the adsorption and activation of N_2 molecules. Specifically, they have demonstrated that ZrS_2 nanofibers with sulfur vacancies can behave as efficient electrocatalyst for ambient N_2 reduction to NH_3 with superb selectivity. Remarkably, In 0.1 mol/L HCl, this ZrS_2 catalyst attains a large NH_3 yield of 30.72 μg h^{-1} mg_{cat}^{-1} and a high faradaic efficiency of 10.33% at −0.35 V and −0.30 V *vs.* RHE, respectively.

5.4. CO_2 reduction reaction

Electrocatalytic CO_2 reduction into a variety of economically valuable chemicals and fuels show a promising way for not only alleviating the "greenhouse effect" but also solve the serious problem of energy shortage [122–124]. However, due to the thermodynamic stability of the CO_2 molecule, a relatively negative potential is normally demanded to activate the molecules, which inevitably results into large energy consumption [125]. To break this bottleneck, the development of efficient and inexpensive electrocatalyst is highly important. In recent years, transition metal compounds, especially for sulfides are reported to be highly active electrocatalysts for CO_2RR. Deep mechanism study also uncovered that the existence of sulfur vacancies in the sulfides can enhance the CO_2 adsorption and the metal sites near the sulfur vacancies are also reported to be conducive to the efficient activation of CO_2 to $CO_2^{\bullet-}$ [126,127]. Additionally, it is also demonstrated that the S-vacancy can also modify the electronic structure of the catalyst, thereby playing a critical role in tailoring the catalytic performance of nanocatalysts. For example, Peng *et al.* [128] reported the synthesis of a composite consisting of CdS with abundant sulfur vacancies and highly conductive CdS to drive electrocatalytic CO_2RR. According to the electrochemical measurements, it is demonstrated that the as-prepared CdS/CNT can catalyze CO_2 reduction to CO with a high faradaic efficiency of 95% due to the *in-situ* generated sulfur vacancies (Figs. 13a-f). More importantly, it is uncovered that the catalytic activity of CO_2RR to CO is associated with the content of sulfur vacancies, with the increase of sulfur vacancies, the catalytic activity of CO_2RR to CO improves substantially and the charge-transfer resistance decreases. Integrated with *in-situ* characterizations and theoretical calculations, it is summarized that the formation of sulfur vacancies can alter the electron density of the catalyst surface and decrease the energy barrier for the conversion of COOH* to CO* (Figs. 13g-i).

Similar results can also be found in Yu's work [129]. To be specific, they have synthesized the S-deficient SnS_{2-x} coupled N-doped hollow carbon spheres (SnS_{2-x}/NHCS) for boosting electrocatalytic CO_2RR. It is disclosed that the existence of sulfur vacancies and energy-level adapted coupling can synergistically decrease the reaction barrier, increase the CO_2 adsorption capacity and affinity with intermediated species, thereby elevating the electrical conductivity and delivering a current density of 35.3 mA/cm^2 at −1.2 V *vs.* RHE and a faradaic efficiency for formate >80%. These advanced researches have confirmed the positive effects of sulfur vacancies on the promotion of electrocatalytic CO_2 performance.

5.5. Oxygen reduction reaction

Sulfur vacancy is also demonstrated to be significant for promoting the electrocatalytic performance towards ORR. Recent years have witnessed the rapid development of ORR electrocatalysts, and many transition metal sulfides with rich sulfur vacancies are reported to be highly active and durable toward ORR. Taking Feng's work as a good example [130], they fabricated the nanocomposite of $NiCo_2S_4$ that uniformly anchored on N, S co-doped rGO with rich sulfur vacancies (S_v-$NiCo_2S_4$/N, S-rGO). Benefitting from numerous active sites and synergistic effect between N, S co-doped rGO and sulfur vacancy-enriched S_v-$NiCo_2S_4$, the as-prepared nanocomposite can exhibit superb catalytic performance towards ORR in 0.1 mol/L KOH solution, with a high half-wave potential of 0.84 V and a low Tafel slope of 43.8 mV/dec. Besides, such nanocatalyst can also exhibit superb catalytic performance towards the electrocatalytic OER performance.

6. Conclusion and perspectives

In summary, we have concluded the recent progress of the sulfur vacancies engineering for boosting electrocatalytic reactions, which include the engineering strategies and the roles of sulfur vacancies played in enhancing catalytic performance. Based on the tremendous efforts devoted, many effective strategies have been proposed for realizing the sulfur vacancy engineering, such as plasma treatment, high-temperature annealing, heteroatom doping, chemical reduction, and electrochemical etching. In addition, it is also summarized that the introduced sulfur vacancies can regulate the electronic structure, tune the active sites, enhance the electron conductivity, and tailor the surface reconstruction. Although the great promise of sulfur vacancy engineering for promoting catalytic performance, some challenging issues should also be addressed before pushing it to practical applications.

First, the characterization technologies of sulfur vacancies should be advanced. In most published works, the vacancy and

defects are usually determined by XPS and EPR measurement, which are superficial characterizations that do not reveal the actual quantities of vacancy. Therefore, the development and employment of more advanced and effective characterization techniques are essential to precisely quantify the exact degree of vacancy in the designed nanomaterials.

As previously demonstrated, sulfur vacancies can be prepared *via* many effective strategies, such as heteroatom doping, plasma and annealing treatment. However, it is still difficult to identify the real role of sulfur vacancy plays in the electrocatalytic reactions since these methods also induce some positive influence on catalytic performance, such as electronic structure modification *via* heteroatom doping, crystal phase change and surface area increased *via* plasma and annealing treatment. Therefore, developing innovative strategies for creating sulfur vacancies without causing other changes in host catalyst is important for investigating the structure-property relationship between sulfur vacancy and catalytic activity.

Most of the researches have identified that introducing sulfur vacancies may post a positive influence on catalytic performance, whereas the relationship between catalytic activity and the concentration of sulfur vacancies is still unclear. Whether a positive relationship between catalytic activity and concentration of sulfur vacancies or not, more efforts should be made.

In addition to catalytic activity, the long-term stability is also a paramount parameter for practical applications. It is well accepted that sulfur vacancy plays a critical role in improving the electrocatalytic activity, but vacancy stability remains poorly understood. Taking electrocatalytic OER as a representative example, when applied a high potential for OER, the precatalyst will be oxidized into high-valence metal oxides or oxyhydroxides. Therefore, determining the dynamic change of sulfur vacancy during electrochemical process is essential to identify the effects on catalytic activity. Also, the influence of sulfur vacancies on the electrocatalytic durability of catalyst is also important, which should be identified.

Overall, the development of sulfur vacancies in the sulfides is a valid strategy to improve catalytic performance, but challenges remain. Therefore, more endeavors should be made to deeply investigate the key roles of sulfur vacancies in tailoring catalytic performance, and more advanced technologies should also be developed to gain a better understanding on the relationship between catalytic performance the concentration of sulfur vacancy.

Declaration of competing interest

The authors declare that they have no known competing financial interests or personal relationships that could have appeared to influence the work reported in this paper.

Acknowledgments

This work was supported by the start-up funding to H. Xu by Changzhou University (No. ZMF22020055), and Advanced Catalysis and Green Manufacturing Collaborative Innovation Center, Changzhou University for financial support. We also thank the Analysis and Testing Center of Changzhou University.

References

[1] H. Xu, J. Yuan, G. He, et al., Coord. Chem. Rev. 475 (2023) 214869.
[2] H. Xu, Y. Zhao, Q. Wang, et al., Coord. Chem. Rev. 451 (2022) 214261.
[3] L. Jin, R. Ji, H. Wan, et al., ACS Catal. 13 (2023) 837–847.
[4] K. Yin, Y. Chao, F. Lv, et al., J. Am. Chem. Soc. 143 (2021) 10822–10827.
[5] H. Xu, B. Huang, Y. Zhao, et al., Inorg. Chem. 61 (2022) 4533–4540.
[6] H. Xu, H. Shang, L. Jin, et al., J. Mater. Chem. A 7 (2019) 26905–26910.
[7] H. Xu, H. Shang, C. Wang, et al., Coord. Chem. Rev. 418 (2020) 213374.
[8] H. Xu, H. Shang, C. Wang, et al., Adv. Funct. Mater. 30 (2020) 2000592.
[9] H. Xu, J. Li, X. Chu, Chem. Rec. 23 (2022) e202200244.
[10] L. Tian, Y. Liu, C. He, et al., Chem. Rec. 23 (2022) e202200213.
[11] L. Tian, H. Chen, X. Lu, et al., J. Colloid Interface Sci. 628 (2022) 663–672.
[12] S. Wang, L. Zhao, J. Li, et al., J. Energy Chem. 66 (2022) 483–492.
[13] H. Xu, H. Shang, C. Wang, et al., Adv. Funct. Mater. 30 (2020) 2006317.
[14] B. Tang, X. Yang, Z. Kang, et al., Appl. Catal. B: Environ. 278 (2020) 119281.
[15] Z. Liu, C. Zhang, H. Liu, et al., Appl. Catal. B: Environ. 276 (2020) 119161.
[16] C. Wang, H. Shang, J. Li, et al., Chem. Eng. J. 420 (2021) 129805.
[17] C. Wang, H. Shang, Y. Wang, et al., J. Mater. Chem. A 9 (2021) 14601–14606.
[18] S. Tang, Y. Zhou, X. Lu, et al., J. Alloys Compds. 924 (2022) 166415.
[19] L. Tian, Z. Huang, W. Na, et al., Nanoscale 14 (2022) 15340–15347.
[20] P. Yan, Q. Liu, H. Zhang, et al., J. Mater. Chem. A 9 (2021) 15586–15594.
[21] Q. Zhang, K. Wang, M. Zhang, et al., CrystEngComm 24 (2022) 5580–5587.
[22] C. Xie, D. Yan, W. Chen, et al., Mater. Today 31 (2019) 47–68.
[23] J. Wan, W. Chen, C. Jia, et al., Adv. Mater. 30 (2018) 1705369.
[24] Y. Tao, J. Yuan, X. Qian, et al., Inorg. Chem. Front. 8 (2021) 2271–2279.
[25] L. Tian, Z. Chen, T. Wang, et al., Nanoscale 15 (2023) 259–265.
[26] Z. Shao, H. Meng, J. Sun, et al., ACS Appl. Mater. Interfaces 12 (2020) 51846–51853.
[27] R. He, X. Huang, L. Feng, Energy & Fuels 36 (2022) 6675–6694.
[28] L. Tian, Z. Huang, X. Lu, et al., Inorg. Chem. 62 (2023) 1659–1666.
[29] J. Jiang, Q. Zhang, A. Wang, et al., Small 15 (2019) 1901791.
[30] C. Tsai, H. Li, S. Park, et al., Nat. Commun. 8 (2017) 15113.
[31] K.H. Kim, K.S. Kim, Y.J. Ji, et al., J. Mater. Chem. C 8 (2020) 1846–1851.
[32] A.Y. Lu, X. Yang, C.C. Tseng, et al., Small 12 (2016) 5530–5537.
[33] C. Zhang, Y. Shi, Y. Yu, et al., ACS Catal. 8 (2018) 8077–8083.
[34] H. Chen, Z. Yu, Y. Hou, et al., Nanoscale 13 (2021) 20670–20682.
[35] G. Zhang, D. Chen, N. Li, et al., Angew. Chem. Int. Ed. 59 (2020) 8255–8261.
[36] L. Li, Z. Qin, L. Ries, et al., ACS Nano 13 (2019) 6824–6834.
[37] H. Su, S. Song, S. Li, et al., Appl. Catal. B: Environ. 293 (2021) 120225.
[38] X. Liu, X. Fan, H. Huang, et al., J. Colloid Interface Sci. 587 (2021) 385–392.
[39] H. Wang, Y. Wang, J. Zhang, et al., Nano Energy 84 (2021) 105943.
[40] Z. Yan, Z. Sun, L. Zhao, et al., Mater. Today Nano 20 (2022) 100261.
[41] Y. Liu, Y. Zhou, X. Zhou, et al., Chem. Eng. J. 407 (2021) 127180.
[42] Y. Ma, D. Leng, X. Zhang, et al., Small 18 (2022) 2203173.
[43] S.S. Chee, C. Oh, M. Son, et al., Nanoscale 9 (2017) 9333–9339.
[44] Y. Zhang, L. Ye, J. Guo, et al., J. Mater. Sci. 56 (2021) 9368–9381.
[45] S.L. Zhang, B.Y. Guan, X.F. Lu, et al., Adv. Mater. 32 (2020) 2002235.
[46] Z. Zhuang, Y. Wang, C.Q. Xu, et al., Nat. Commun. 10 (2019) 4875.
[47] J. Feng, F. Lv, W. Zhang, et al., Adv. Mater. 29 (2017) 1703798.
[48] Y. Li, J. Qian, M. Zhang, et al., Adv. Mater. 32 (2020) 2005802.
[49] K. Zhang, B.M. Bersch, J. Joshi, et al., Adv. Funct. Mater. 28 (2018) 1706950.
[50] G. Liu, D. Luo, R. Gao, et al., Small 16 (2020) 2001089.
[51] H. Li, C. Tsai, A. Koh, et al., Nat. Mater. 15 (2015) 48.
[52] H. Li, M. Du, M.J. Mleczko, et al., J. Am. Chem. Soc. 138 (2016) 5123.
[53] L. Tian, X. Pang, H. Xu, et al., Inorg. Chem. 61 (2022) 16944–16951.
[54] J. Long, Q. Yao, X. Zhang, et al., Appl. Catal. B: Environ. 320 (2023) 121989.
[55] L. Liang, W. Gu, Y. Wu, et al., Adv. Mater. 34 (2022) 2106195.
[56] T. Wang, X. Li, Y. Pang, et al., Chem. Eng. J. 425 (2021) 131491.
[57] H. Yu, T. Zhou, Z. Wang, et al., Angew. Chem. Int. Ed. 60 (2021) 12027–12031.
[58] S. Huang, Z. Jin, P. Ning, et al., Chem. Eng. J. 420 (2021) 127630.
[59] W. Deeloed, T. Priamushko, J. Cizek, et al., ACS Appl. Mater. Interfaces 14 (2022) 23307–23321.
[60] X. Li, K. Zheng, J. Zhang, et al., ACS Omega 7 (2022) 12430–12441.
[61] J. Wu, W. Zhong, C. Yang, et al., Appl. Catal. B: Environ. 310 (2022) 121332.
[62] Z. Li, X. Xu, X. Lu, et al., J. Colloid Interface Sci. 615 (2022) 273–281.
[63] X. Zheng, J. Yang, Z. Xu, et al., Angew. Chem. Int. Ed. 61 (2022) 202205946.
[64] J. Chang, G. Wang, Z. Yang, et al., Adv. Mater. 33 (2021) 2101425.
[65] Q. Chang, Y. Jin, M. Jia, et al., J. Colloid Interface Sci. 575 (2020) 61–68.
[66] M. Shamloofard, S. Shahrokhian, Nanoscale 13 (2021) 17576–17591.
[67] T. Zhang, W. Zong, Y. Ouyang, et al., Adv. Fiber Mater. 3 (2021) 229–238.
[68] H. Song, T. Li, T. He, et al., Chem. Eng. J. 450 (2022) 138115.
[69] Y. Sun, Y. Li, Y. Qin, et al., Chem. Eur. J. 26 (2020) 4032–4038.
[70] H. Xu, J. Cao, C. Shan, et al., Angew. Chem. Int. Ed. 57 (2018) 8654–8658.
[71] C. Fan, X. Wu, M. Li, et al., Chem. Eng. J. 431 (2022) 133829.
[72] X. Li, C. Wang, S. Zheng, et al., J. Colloid Interface Sci. 624 (2022) 443–449.
[73] L. An, Y. Hu, J. Li, et al., Adv. Mater. 34 (2022) e2202874.
[74] Y. Li, C. Jiang, Y. Yang, et al., Appl. Surf. Sci. 604 (2022) 154470.
[75] H. Man, J. Feng, S. Wang, et al., Cell Rep. Phys. Sci. 3 (2022) 101059.
[76] L. Zhang, J. Wang, K. Jiang, et al., Angew. Chem. Int. Ed. 61 (2022) 2214794.
[77] F. Wu, R. Yang, S. Lu, et al., ACS Energy Lett. 7 (2022) 4198–4203.
[78] T.I. Singh, G. Rajeshkhanna, U.N. Pan, et al., Small 17 (2021) e2101312.
[79] L. Li, L. Bu, B. Huang, et al., Adv. Mater. 33 (2021) 2105308.
[80] Y. Zhou, H.J. Fan, ACS Mater. Lett. 3 (2020) 136–147.
[81] S. Fan, J. Zhang, Q. Wu, et al., J. Phys. Chem. Lett. 11 (2020) 3911–3919.
[82] S. Anantharaj, S. Noda, Small 16 (2020) e1905779.
[83] J. Zhang, X. Mao, S. Wang, et al., Angew. Chem. Int. Ed. 61 (2022) 202116867.
[84] S. Anantharaj, Curr. Opin. Electrochem. 33 (2022) 100961.
[85] H. Xu, Y. Zhao, G. He, et al., Int. J. Hydrogen Energy 47 (2022) 14257–14279.
[86] J. Zhang, J. Le, Y. Dong, et al., Sci. China Chem. 65 (2021) 87–95.
[87] L. Li, P. Wang, Q. Shao, et al., Chem. Soc. Rev. 49 (2020) 3072–3106.
[88] T. Zhu, J. Huang, B. Huang, et al., Adv. Energy Mater. 10 (2020) 2002860.
[89] L. Zhang, Y. Lei, D. Zhou, et al., Nano Res. 15 (2021) 2895–2904.
[90] M. Wang, J.Q. Wang, C. Xi, et al., Small 17 (2021) 2100203.
[91] Z.W. Wei, H.J. Wang, C. Zhang, et al., Angew. Chem. Int. Ed. 60 (2021) 16622–16627.
[92] J. Li, J. Hu, M. Zhang, et al., Nat. Commun. 12 (2021) 3502.

[93] G. Li, D. Zhang, Q. Qiao, et al., J. Am. Chem. Soc. 138 (2016) 16632–16638.
[94] H. Li, S. Wang, H. Sawada, et al., ACS Nano 11 (2017) 3392–3403.
[95] K. Zhang, Y. Duan, N. Graham, et al., Appl. Catal. B: Environ. 323 (2023) 122144.
[96] Z. Cai, P. Wang, J. Zhang, et al., Adv. Mater. 34 (2022) 2110696.
[97] S. Xu, Q. Huang, J. Xue, et al., Inorg. Chem. 61 (2022) 8909–8919.
[98] O.N. Avci, L. Sementa, A. Fortunelli, ACS Catal. 12 (2022) 9058–9073.
[99] K. Chang, D.T. Tran, J. Wang, J. Mater. Chem. A 10 (2022) 3102–3111.
[100] R. Abazari, S. Sanati, A. Morsali, Inorg. Chem. 61 (2022) 3396–3405.
[101] H. Xu, C. Wang, G. He, et al., Inorg. Chem. 61 (2022) 14224–14232.
[102] Q. Chen, Q. Zhang, H. Liu, et al., Small 17 (2021) 2007858.
[103] H. Liu, Z. Liu, F. Wang, L. Feng, Chem. Eng. J. 397 (2020) 125507.
[104] R. Madhu, S.S. Sankar, K. Karthick, et al., Inorg. Chem. 60 (2021) 9899–9911.
[105] Z.P. Wu, H. Zhang, S. Zuo, et al., Adv. Mater. 33 (2021) 2103004.
[106] Y. Cong, S. Huang, Y. Mei, et al., Chem. Eur. J. 27 (2021) 15866–15888.
[107] Y. Li, K. Jiang, J. Yang, et al., Small 17 (2021) 2102159.
[108] R. He, C. Wang, L. Feng, Chin. Chem. Lett. 34 (2023) 107241.
[109] X. Miao, L. Wu, Y. Lin, et al., Chem. Commun. 55 (2019) 1442–1445.
[110] M. Li, L. Feng, Chin. J. Struct. Chem. 41 (2022) 2201019–2201024.
[111] H. Xu, H. Shang, C. Wang, et al., Appl. Catal. B: Environ. 265 (2020) 118605.
[112] Q. Wang, H. Xu, X. Qian, et al., Appl. Catal. B: Environ. 322 (2023) 122104.
[113] L. Zhao, Y. Xiong, X. Wang, et al., Small 18 (2022) 2106939.
[114] Y. Wang, D. Wang, Y. Li, Adv. Mater. 33 (2021) 2008151.
[115] M. Liu, S. Yin, T. Ren, et al., ACS Appl. Mater. Interfaces 13 (2021) 47458–47464.
[116] P.Y. Liu, K. Shi, W.Z. Chen, et al., Appl. Catal. B: Environ. 287 (2021) 119956.
[117] M. Arif, G. Yasin, L. Luo, et al., Appl. Catal. B: Environ. 265 (2020) 118559.
[118] J. Wang, B. Huang, Y. Ji, et al., Adv. Mater. 32 (2020) 1907112.
[119] K. Chu, H. Nan, Q. Li, et al., J. Energy Chem. 53 (2021) 132–138.
[120] C. Li, R. Xu, S. Ma, et al., Chem. Eng. J. 415 (2021) 129018.
[121] T. Xu, D. Ma, T. Li, et al., Chem. Commun. 56 (2020) 14031–14034.
[122] J. Wang, C. Cheng, B. Huang, et al., Nano Lett. 21 (2021) 980–987.
[123] Y. Wang, C. Li, Z. Fan, et al., Nano Lett. 20 (2020) 8074–8080.
[124] N. Zhang, F. Zheng, B. Huang, et al., Adv. Mater. 32 (2020) 1906477.
[125] Y. Feng, H. Yang, Y. Zhang, et al., Nano Lett. 20 (2020) 8282–8289.
[126] R. Cui, Q. Yuan, C. Zhang, et al., ACS Catal. 12 (2022) 11294–11300.
[127] H. Tao, X. Sun, S. Back, et al., Chem. Sci. 9 (2018) 483–487.
[128] B. Qin, Y. Li, H. Wang, et al., Nano Energy 60 (2019) 43–51.
[129] Y. Li, W. Niu, T. Chen, et al., Appl. Catal. B: Environ. 321 (2023) 122037.
[130] X. Feng, Q. Jiao, Q. Li, et al., Electrochim. Acta 331 (2020) 135356.